ELSEVIER

International Journal of Inorganic Materials 2 (2000) 601–608

International Journal of Inorganic Materials

Coexistence of superconductivity and ferromagnetism in 1212-$Ru_{1-x}M_xSr_2GdCu_2O_8$ (M=Ti, V, Nb)

Sylvie Malo[a], Donggeun Ko[a], Job T. Rijssenbeek[a], Antoine Maignan[b,*], Denis Pelloquin[b], Vinayak P. Dravid[c], Kenneth R. Poeppelmeier[a]

[a]*Department of Chemistry and the Science and Technology Center for Superconductivity, Northwestern University, Evanston, IL 60208, USA*
[b]*Laboratoire CRISMAT-ISMRA, UMR 6508, Université de Caen, Caen, France*
[c]*Department of Material Science and Engineering and the Materials Research Center, Northwestern University, Evanston, IL 60208, USA*

Dedicated to Professor Bernard Raveau on the occasion of his 60th Birthday

Abstract

The coexistence of superconductivity and ferromagnetism in 1212-$RuSr_2GdCu_2O_8$ is unique among high-T_c materials. Samples of $Ru_{1-x}M_xSr_2GdCu_2O_8$, with M=Ti, V and Nb; and $0 \leq x \leq 1$, were prepared to elucidate the role of the RuO_2 planes in this interesting layered 1212 cuprate. The solubility ranges of M=Ti and V are limited to $x<0.15$ whereas that of Nb extends to full substitution. In all cases superconductivity is lost at higher substitution levels ($x>0.2$), however with vanadium substitution the T_c increases from 20 K to 25 K. The ferromagnetism of the RuO_2 layers is dramatically affected by the electronic configuration of the substituting ion, weakened for M=Ti and Nb and enhanced for M=V. These results indicate that the superconductivity and ferromagnetism are intimately linked to the layered architecture of this 1212 structure.

Keywords: D. Superconductivity; Ferromagnetism; Cuprates; Ruthenium

1. Introduction

Bi-dimensional CuO_2 planes are the common structural feature of all superconducting cuprates. Their layering along one direction results from oxygen vacancies and/or from several types of intergrowths between the CuO_2 planes and connecting layers such as CuO chains in $YBa_2Cu_3O_7$ or NaCl-type layers in Hg, Tl, Pb, Bi based superconductors. The connecting layer can act as a charge reservoir by supplying the carriers necessary for the superconductivity of the CuO_2 planes. These connecting layers, which are less conductive than the CuO_2 planes [1], govern the *c* axis resistivity of cuprates. For instance, the out-of-plane resistivity (ρ_c) increases as one goes from $YBa_2Cu_3O_7$ with CuO_4 square chains as blocking layer, through single-layered compounds such as Tl-12($n-1$)*n* or Hg-12($n-1$)*n* where n is the number of CuO_2 planes [2–4], to $Bi_2Sr_2CaCu_2O_8$ with three NaCl-type layers. Accordingly, ρ_c provides a measure of the pinning properties as the superconductor becomes more anisotropic [5]. Nevertheless, the critical temperature (T_{crit}) of these superconductors is not correlated to this dimensional aspect as evidenced by the similar T_{crit}s of optimally doped $YBa_2Cu_3O_{7-\delta}$ and $Bi_2Sr_2CaCu_2O_{8+\delta}$.

The recent reports of superconductivity for ruthenium based cuprates $RuSr_2LnCu_2O_8$ and $RuSr_2(Ln_{1+x}Ce_{1-x})Cu_2O_{10}$ [6–10] have added a new kind of connecting block, the [$SrRuO_3$] plane, to those previously known. But in addition to its role as a charge reservoir, the RuO_2 plane is also a magnetic layer. The physical properties of these new layered phases are very intriguing since superconductivity and planar ferromagnetism coexist, and contrasts with other mixed Ru/Cu oxides which display semiconductor-like behavior and weak ferromagnetism [11,12]. This emphasizes the consequence of the layering of the CuO_2 and RuO_2 planes on the properties. The superconductivity of this material can only be explained if some carriers are created in the CuO_2 planes by some Ru^{5+}/Ru^{4+} mixed valency and if the ferromagnetism of the majority Ru^{5+} species (low spin-

*Corresponding author. Tel.: +33-231-452-634; fax: +33-231-951-600.

E-mail address: antoine.maignan@ismra.fr (A. Maignan).

1466-6049/00/$ – see front matter
PII: S1466-6049(00)00075-1

states $4d^3$, $S=1/2$) is developed in the (a,b) planes to avoid pair-breaking [8,10].

Consequently, cationic substitution for ruthenium should provide some important insights into the understanding of the coexistence of superconductivity and ferromagnetism in Ru-1212. We have chosen to substitute ruthenium with niobium and titanium for their d^0 configurations in 5+ and 4+ oxidation states, respectively, which should strongly weaken the magnetic interactions in the RuO_2 magnetic planes. In addition, vanadium, which can exhibit V^{4+}/V^{5+} mixed-valency, may mimic the same spin as low-spin Ru^{4+}/Ru^{5+}, i.e. $S=1/2$ for V^{4+} and Ru^{5+} and $S=0$ for V^{5+} and Ru^{4+}.

Several series of polycrystalline $Ru_{1-x}M_xSr_2GdCu_2O_8$ samples with M=Ti, V, and Nb; and $0\leq x\leq 1$ have been prepared. The solubility range of these elements has been found to depend on their oxidation states and seems also to be connected to their coordination environment. We show that the substitutions of these elements for ruthenium can induce opposite effects on its magnetic response, i.e. a weakening or reinforcement of the ferromagnetic properties depending on the element. More importantly, for low x values in $Ru_{1-x}M_xSr_2GdCu_2O_8$ ($x<0.15$), the superconducting critical temperature T_{crit} and the Curie temperature T_{Cur} are not directly connected in these 1212 type compounds. The possibility of obtaining fully oxygenated and pure samples after a one-step synthesis process in air together with an unusual sensitivity of the diamagnetic response to low magnetic fields could yield new applications for the superconducting cuprates.

2. Experimental

The $Ru_{1-x}M_xSr_2GdCu_2O_8$ samples with M=Ti, V and Nb have been synthesized by solid-state reactions performed in air. Stoichiometric amounts of $SrCO_3$, Gd_2O_3, CuO, RuO_2 and $V_2O_5/Nb_2O_5/TiO_2$ powders were thoroughly ground in an agate mortar, pressed into pellets and then sintered. The calcination was first made at 950°C for 12 h in order to achieve decomposition of the carbonates and then, without interruption, the temperature was increased directly to 1040°C and maintained for 72 h. The samples were cooled to room temperature over a period of 12 h. Annealings under high oxygen pressure (150 atm.) at 500°C for 12 h have also been performed in order to refill possible oxygen vacancies.

Powder X-ray patterns were recorded with a Rigaku diffractometer using Ni-filtered Cu K_α radiation. Two-theta scans were conducted from 10° to 80° with 0.02° step size and 2 s collection time.

For the electron microscopy study, the samples were prepared by crushing a small ceramic piece in alcohol. The small crystallites were deposited on a holey carbon film supported by a Ni or nylon grid. The electron diffraction (ED) was carried out with an 8100 Hitachi electron microscope working at 200 kV. The EDS analyses were performed on numerous crystallites of the powder samples with a KEVEX analyzer mounted on this electron microscope.

The oxygen contents of the $Ru_{1-x}M_xSr_2GdCu_2O_8$ samples were determined by hydrogen reduction (7% H_2/He) through thermogravimetric analysis (TGA). The samples were heated to 900°C at the rate of 10°C/min, then isothermally maintained for 10 h, and cooled down to room temperature at the same rate.

Magnetization measurements were performed on small pieces of samples with a Quantum Design DC SQUID magnetometer. Because the magnetization of the $Ru_{1-x}M_xO_2$ layers has been found to dramatically suppress the superconductivity of CuO_2 layers, careful consideration should be given to the remnant magnetic field of ~1 Oe which may destroy the superconductivity. Thus, only high-field measurements have been performed in this magnetometer to characterize the magnetic behavior of the Gd ions and the RuO_2 planes.

The superconductivity has been characterized by AC susceptibility measurements performed with an AC-7000 Lake Shore Susceptometer. AC magnetic fields ranging from 10^{-2} to 3 Oe with a constant frequency of 133 Hz have been applied to measure the complex susceptibility (χ', χ'') of the samples. No static field was applied so that the virgin superconducting coil ensured a true zero-field cooled (zfc) process on the samples down to liquid helium temperature prior to data collection. No demagnetization corrections have been performed. The same instrument was used to measure the T dependence of the samples resistance (R). Bars with typical dimensions of $10\times2\times2$ mm^3 were cut from pellets. Gold wires were attached to the sample using silver paste. The measurements were performed using a classical four-probe method. After a ZFC process, the resistance values were collected upon warming using AC currents ranging from 10^{-1} to 10 mA. $R(T)$ curves have also been registered in 10^4 Oe.

3. Results

3.1. Structural characterizations

From powder X-ray diffraction and energy dispersive spectroscopic (EDS) analyses coupled to electron diffraction (ED), the solubility behavior is shown to differ between that of Ti and V, and Nb. First, as shown by the X-ray diffractograms in Fig. 1, a complete solid solution is found from Ru-1212 to Nb-1212, which indicates that Ru exhibits mainly a pentavalent oxidation state similar to Nb. Refined tetragonal cell parameters are found to increase as x increases in $Ru_{1-x}Nb_x$. This evolution is expected if one compares the larger ionic radius [13] of Nb^{5+}, 0.64 Å, against 0.565 Å for Ru^{5+}. The cell parameters of the Nb- and Ru-1212 end-members are very close to those already

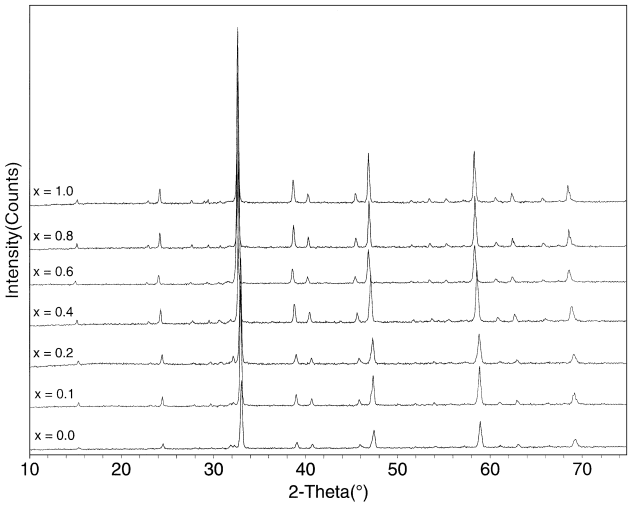

Fig. 1. X-ray diffractograms for the $Ru_{1-x}Nb_xSr_2GdCu_2O_8$ samples. For sake of clarity, the diffractograms have been intentionally shifted along the intensity axis. Values of x are labeled on the graph.

reported [6–9,14]. Thermo-gravimetric analysis yields an oxygen content of eight, consistent with six-fold coordination of Ru^{5+} and Nb^{5+}. It should be emphasized that this complete solubility range $Ru_{1-x}Nb_xSr_2GdCu_2O_8$ with $0 \leq x \leq 1$, observed for our samples, differs from the partial solubility of Ru for Nb, corresponding to $0.5 \leq x \leq 1$, reported by Hellebrand et al. [15] for $Ru_{1-x}Nb_xSr_2LnCu_2O_8$ with Ln = Sm. The use of dissimilar lanthanides may be at the origin of this discrepancy. The results obtained for the whole $Ru_{1-x}Nb_x$ series will be detailed elsewhere [16].

A second kind of behavior is encountered for titanium and vanadium, which exhibit relatively small solubility ranges. In their diffraction patterns, impurity peaks, assigned to $SrRuO_3$ and $SrMO_3$ (M = Ti or V) are observed for $x \geq 0.10$ (Fig. 2a,b). The EDS analyses performed on the $Ru_{1-x}M_x$ ($x = 0.1$, 0.2; nominal content) samples confirm the partial substitution of the different M cations for ruthenium. However, even for this low nominal content of foreign cations the solubility is limited to approximately 0.05 for vanadium and 0.15 for titanium. Moreover, for M = Ti and V, the results of the EDS analyses suggest that the Sr/(Ru + M) ratio is slightly greater than two, which may indicate the presence of some copper on the ruthenium site. This deviation is not observed for the M = Nb samples. Additional HREM studies will be performed in order to elucidate the existence of possible complex structural defects, or nucleation of new phases, in the vanadium substituted samples.

The substitution of both Ti and V is compensated by a slight decrease in the oxygen content. This is shown in Table 1, where the values determined by TGA for the oxygen content and the cell parameters of the pure Ru and three $Ru_{0.9}M_{0.1}$-1212 samples are reported. In agreement with previous work [7], no change in the oxygen content

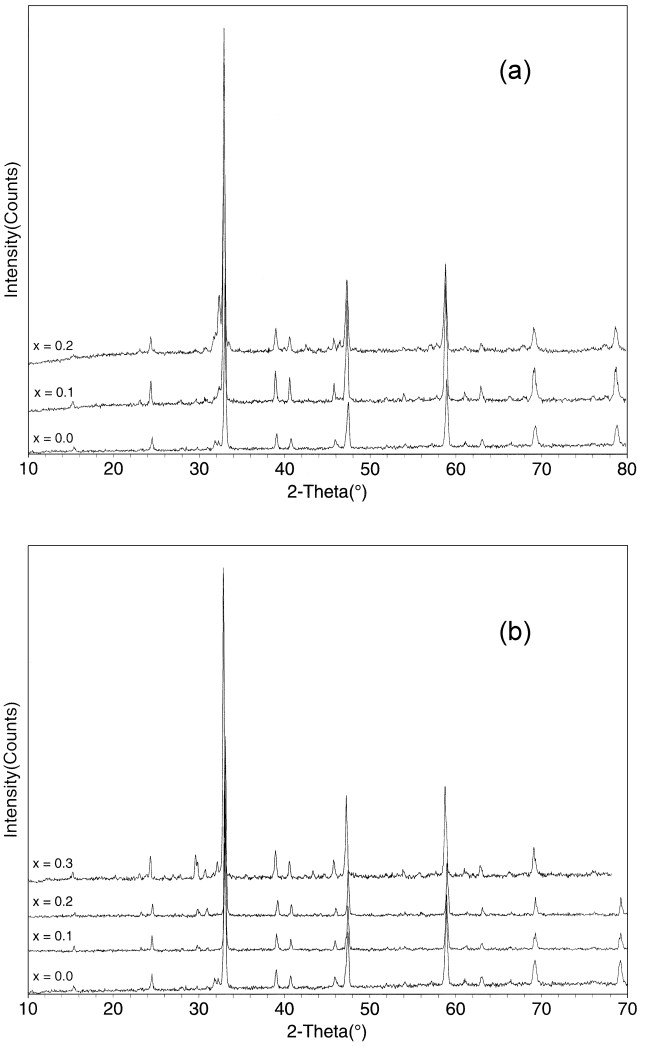

Fig. 2. X-ray diffractograms for the $Ru_{1-x}M_xSr_2GdCu_2O_8$ samples. M = Ti (a) and M = V (b). For sake of clarity, the diffractograms have been intentionally shifted along the intensity axis. Values of x are labeled on the graphs.

can be detected for the high P_{O2} treated samples. The comparison of the c cell parameters for the three $Ru_{0.9}M_{0.1}Sr_2GdCu_2O_8$ samples gives the relation $c_{Nb} > c_{Ti} > c_V$, in agreement with their respective ionic radii, $r_{Nb^{5+}}$ (0.64 Å) $> r_{Ti^{4+}}$ (0.605 Å) $> r_{V^{4+}}$ (0.58 Å) $> r_{V^{5+}}$ (0.54 Å). Nevertheless, the a parameter does not match with the cationic radius evolution especially for vanadium. This may reflect the tendency of this cation to adopt a tetrahedral coordination as already reported in (Hg,V)-based superconductors [17,18]. This would explain the low solubility limit of this cation for Ru, which is not expected considering the similarities of their mixed-valency.

The peculiar role of V on the Ru-1212 structure is demonstrated by the electron diffraction (ED) study performed on the as-synthesized samples corresponding to the nominal formula $Ru_{0.9}M_{0.1}Sr_2GdCu_2O_8$ (M = Ru, Nb, Ti and V). The ED patterns of the four different samples show a set of intense reflections characteristic of the tetragonal subcell ($a \approx a_p \approx 3.9$ Å and $c \approx 3a_p \approx 11.6$ Å)

Table 1
Cell parameters (P4/mmm space group) of the Ru-1212 phase and of $Ru_{0.9}M_{0.1}Sr_2GdCu_2O_{8-\delta}$ samples (nominal composition; as-prepared)[a]

M	a (Å)	c (Å)	r (Å)	δ	Ru_x	Sr/(Ru+M)
$Ru^{5+/4+}$	3.8373(3)	11.566(2)	0.565/0.62	0.06(2)	1.0	2.00
Ti^{4+}	3.8376(1)	11.561(1)	0.601	0.09(2)	0.95	2.22
Nb^{5+}	3.8406(2)	11.567(1)	0.64	0.07(2)	0.89	2.00
$V^{5+/4+}$	3.8640(2)	11.545(1)	0.54/0.58	0.17 (2)[b]	0.95	2.15

[a] The cationic radius values (VI coordinate), r, come from Ref. [13]. The oxygen deficiency δ is also given. No significant change is observed after the high O_2-pressure treatments.
[b] Calculated assuming V_2O_3 is the resulting product of the TGA reduction.

without any reflection conditions. These results are in agreement with previous structural determination based on X-ray data for the Ru-1212 phase [6].

However, in all investigated as-synthesized Ru-1212 and RuM-1212 samples, barely visible extra reflections are observed at positions 1/2 1/2 0 in the [001] ED patterns which involve a doubled cell with $a \approx a_p\sqrt{2}$. These extra reflections have also been observed in as-synthesized Ru-1212 samples by McLaughlin et al. [7] and after annealing by Pringle et al. [10]. However, as we could not observe any extra peak in the X-ray diffractogram, we have not considered a larger cell for the refinement of the lattice parameters which have been obtained by using the $a_p \times a_p \times 3a_p$ unit cell.

The mixed Ru/Ti and Ru/Nb samples exhibit the same set of intense reflections as the Ru-1212 with systematic diffuse satellites along c^* on the [120] patterns that are correlated to the tilting of the RuO_6 octahedra in an $a^0\ a^0\ c^+$ fashion [19]. This suggests a similar octahedral coordination for Nb, Ti and Ru without any ordering phenomenon in the mixed layer $Ru_{1-x}M_xO_2$. We have not observed a doubling of the c parameter with space group I4/mcm as evidenced by Vybornov et al. [14] for the niobium based 1212, $NbSr_2SmCu_2O_8$, and Rey et al. for $NbBa_2LaCu_2O_8$ [20].

In some microcrystals of these three samples (Ru, $Ru_{1-x}Nb_x$ and $Ru_{1-x}Ti_x$), 90° oriented domains are observed. The existence of these domains is observed in the [001] ED patterns; an example is shown in Fig. 3. However, no clear relationship between the twinning phenomena and the physical properties has been established.

In contrast to Ti and Nb substituted samples, the substitution of vanadium for ruthenium leads to an additional structural modification. On all (hk0) planes, there exist extra reflections which generally involve a doubling of the c parameter. This is illustrated by the [100] and [110] ED patterns given in Fig. 4a,b, respectively. These additional reflections are streaked along c^* and are more pronounced in samples of nominally greater vanadium content. The patterns for Ru-1212 are also shown for comparison.

Physical properties measurements have been performed only on samples with nominal compositions of $x=0.1$ and $x=0.2$ with M=Ti, and of $x=0.1$ with M=V, because the solubility limits of Ti and V are about 15% and 5%, respectively.

3.2. Physical properties: effect of the substitutions on the Curie and superconducting critical temperatures

The structure of the superconducting pristine compound, $RuSr_2GdCu_2O_8$, with $T_{crit}=15$–40 K [7,8], has been previously shown to consist of the regular intergrowth of superconducting CuO_2 bilayers with RuO_2 layers in which the Ru cations are ferromagnetically coupled with $T_{Cur}=$ 133–136 K. The latter value is also obtained for the present Ru-1212 oxide as shown from the T dependent magnetization curve registered in 10^3 Oe (Fig. 5, curve a) from which T_{Cur} is determined as the inflection point of the ferromagnetic transition. One can also see on this curve the absence of diamagnetism at the lowest temperatures for this magnetic field value. This point, i.e. the high sensitivity of superconducting diamagnetism to magnetic field, will be discussed later.

As expected, the substitution of d^0 cations for Ru^{5+}, which break the Ru–O–Ru ferromagnetic pathways, decreases the Curie temperature and the magnetization values. This can be seen in Fig. 5 by comparing the $Ru_{0.8}Ti_{0.2}$ and $Ru_{0.8}Nb_{0.2}$ curves (curves b and c) to the Ru-1212 curve (curve a) which show $T_{Cur}\sim 120$ K and 135

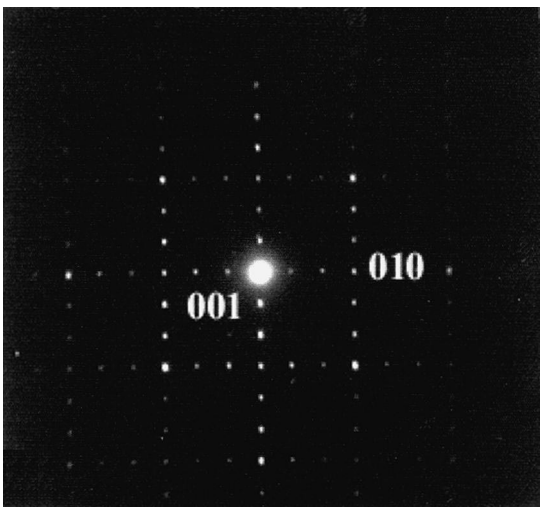

Fig. 3. [100] ED pattern of a twinned $RuSr_2GdCu_2O_8$ micro-crystal.

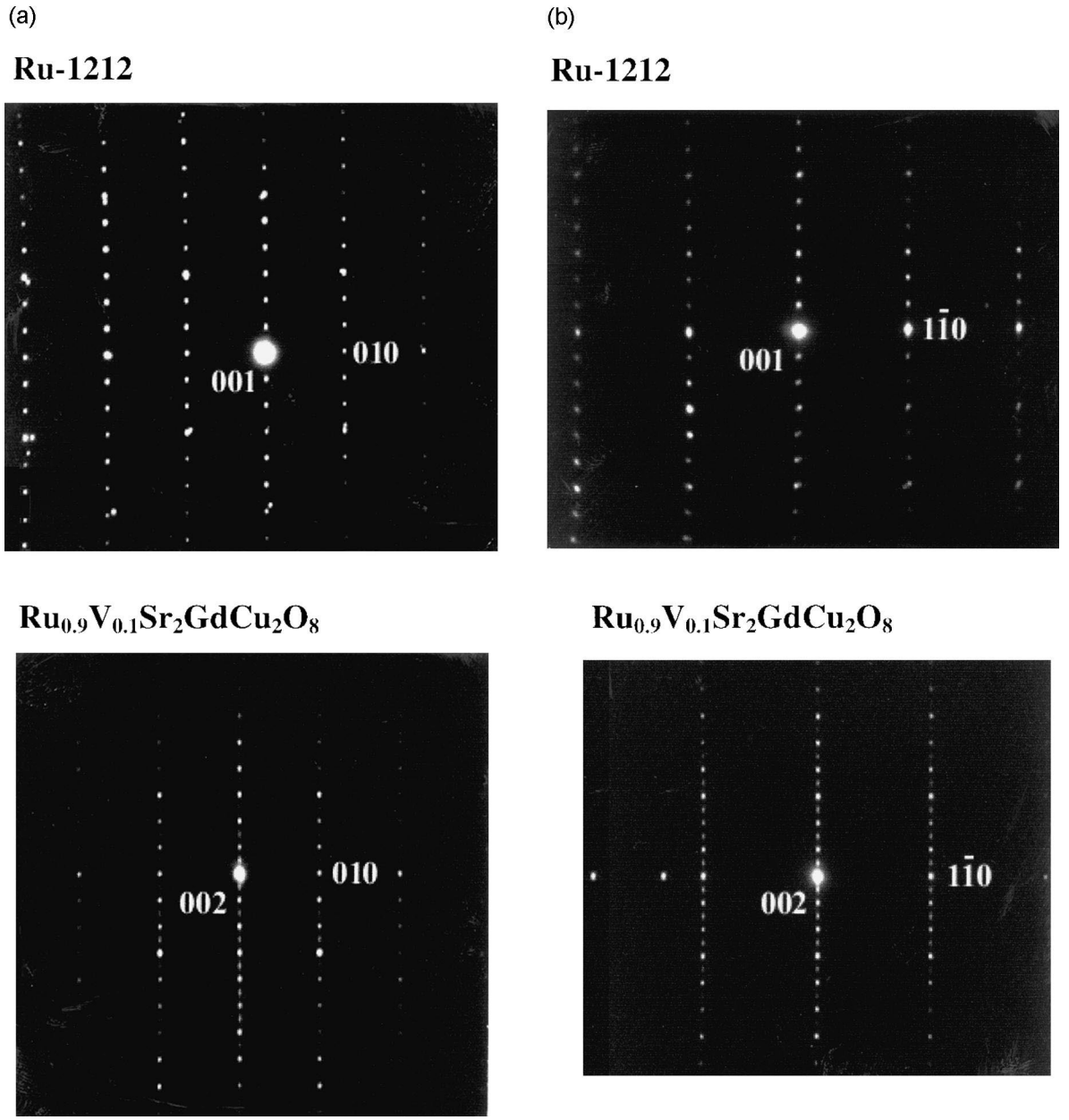

Fig. 4. ED patterns of $Ru_{0.9}V_{0.1}Sr_2GdCu_2O_8$ and Ru-1212, for comparison: (a) [100] and (b) [110].

K, respectively. More than the oxidation state, either 4+ or 5+, the spin configuration of the substituted M cation affects the magnetism of the RuO_2 layers. This result is strongly supported by the data collected for M=V and $x=0.1$ (curve d in Fig. 5) showing that T_{Cur} is increased by about 10 K in comparison with the Ru-1212 phase. The M(T) curves for the vanadium-substituted (curve d) and pure Ru-1212 (curve a) samples merge for the lowest temperature as shown from the similar M values at 5 K. Finally, all the M(T) curves show a large magnetization increase for the lowest temperature which is the result of the paramagnetic contribution of the Gd ion.

In order to confirm the different effect of Nb (or Ti) and V on the ferromagnetism, M(H) loops have also been recorded. The M(H) curves registered at 5 K (Fig. 6) emphasize the peculiar role of V in comparison to the d^0 cations – the V doped and Ru-1212 M(H) curves are superimposed whereas the curve for Ti and Nb lie below. For M=Ti, the magnetization difference is approximately 1 μ_B for H=55 kOe which corresponds approximately to the disappearance of the Ru magnetic moment in the RuO_2 planes [Ru^{5+} (d^3, $S=1/2$)].

To summarize, the M(T) and M(H) curves for the pure Ru-1212 and substituted $Ru_{0.8}M_{0.2}Sr_2GdCu_2O_8$ samples show that the ferromagnetism of the RuO_2 layer can be strongly modified, that is enhanced or weakened, depending on the magnetic nature of the substituting cation. If the ferromagnetism and superconducting order parameters

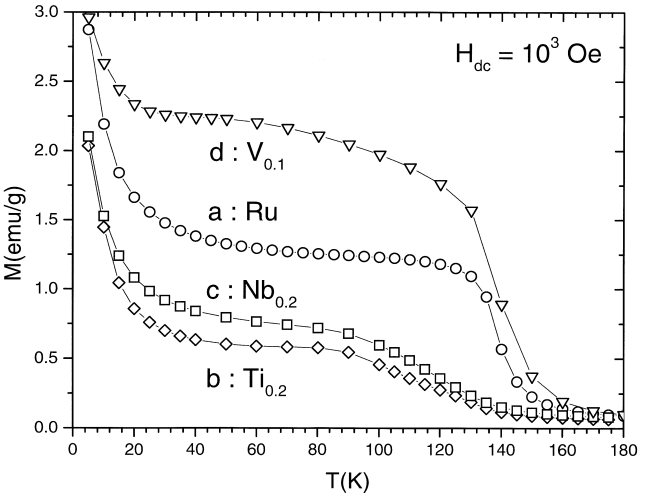

Fig. 5. T dependent magnetization (M) registered upon warming in 10^3 Oe after a zero-field-cooling process (zfc) at 5 K: $RuSr_2GdCu_2O_8$ (a), $Ru_{0.8}Ti_{0.2}Sr_2GdCu_2O_8$ (b), $Ru_{0.8}Nb_{0.2}Sr_2GdCu_2O_8$ (c), and $Ru_{0.9}V_{0.1}Sr_2GdCu_2O_8$ (d).

compete in Ru-1212, one would expect to increase T_{crit} by weakening the ferromagnetism (M=Ti and Nb) and vice-versa (M=V). In the following, the superconductivity characterizations show that this is not the case. Whatever the M substituted cation is, superconductivity is always suppressed above $x=0.20$ in $Ru_{1-x}M_x$, whereas the Curie temperature is observed to increase or decrease. This is shown in Fig. 7, where the real part of the complex susceptibility χ' ($H_{ac}=10^{-2}$ Oe) versus temperature curves are reported for the as-prepared samples. The $\chi'(T)$ curve of the Ru-1212 and those of the $Ru_{0.9}M_{0.1}$-1212 exhibit a diamagnetic transition characteristic of superconductivity. The presence of the foreign cation may be at the origin of a charge localization effect in the mixed $Ru_{1-x}M_xO_2$ layer, preventing any carrier delocalization between the adjacent RuO_2 and CuO_2 planes.

More interestingly, the $\chi'(T)$ curves registered for lower

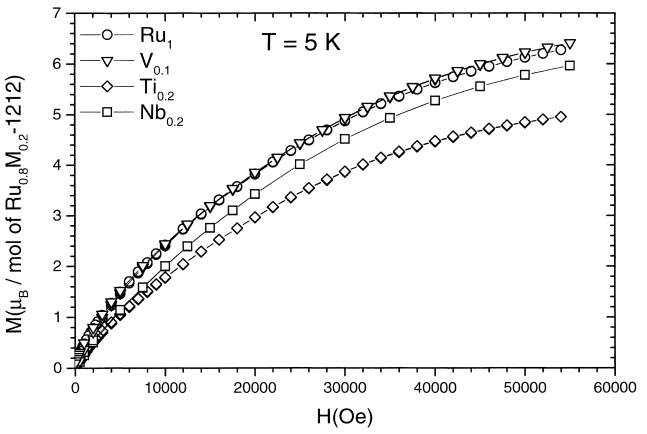

Fig. 6. $M(H)_{5K}$ curves for Ru-1212 (○), $Ru_{0.8}V_{0.1}$-1212 (▽), $Ru_{0.8}Ti_{0.2}$-1212 (◇) and $Ru_{0.8}Nb_{0.2}$-1212 (□).

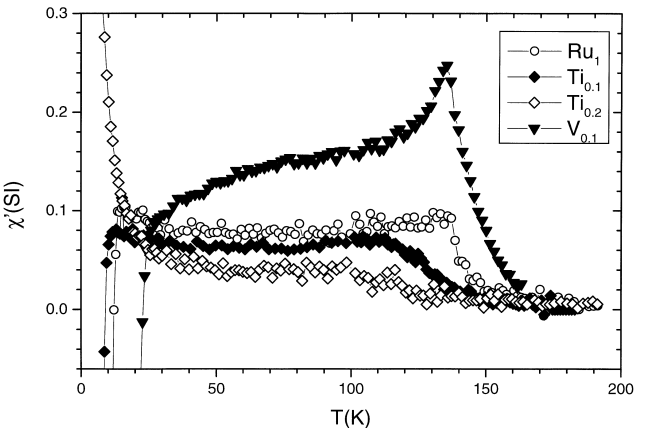

Fig. 7. Real part (χ') of the AC susceptibility as a function of temperature registered with $H_{ac}=10^{-2}$ Oe and $f=133$ Hz. $Ru_{1.0}$ (○), $Ru_{0.9}Ti_{0.1}$ (♦), $Ru_{0.8}Ti_{0.2}$ (◇), and $Ru_{0.9}V_{0.1}$ (▼).

doping levels (nominally $x=0.10$) (Fig. 8) demonstrate that the superconductivity exists independently of the effect of the substituting elements on ferromagnetism. The T_{crit}s are improved slightly by the oxygen pressure annealing treatments, suggesting that small variations of the oxygen content affect the superconductivity. It is remarkable that the highest T_{crit} is exhibited for the V-substituted sample with an onset at 19 K, whereas the T_{crit}s of Ti and Nb, 9 K and 13 K, respectively, are smaller than the T_{crit} value of 15 K for Ru-1212. The temperature-dependent resistivity curves of Ru-1212 and $Ru_{0.9}V_{0.1}$-1212 (Fig. 9) confirm the improvement of the critical temperature from 20 K to 25 K, respectively, by the V substitution while simultaneously with this change the ferromagnetism is reinforced.

It is also interesting that the superconductivity of these 1212 rutheno-cuprates is very sensitive to the AC magnetic field magnitude. The excluded volume fraction is de-

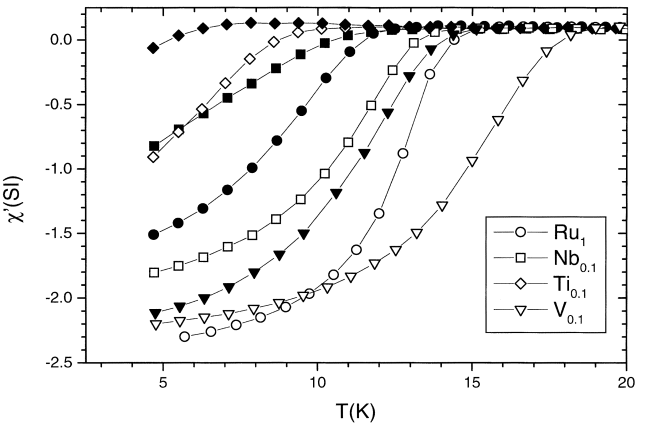

Fig. 8. $\chi'(T)$ ($H_{ac}=10^{-2}$ Oe and $f=133$ Hz) curves: enlargement of the superconducting region. Solid and empty symbols represent the as-prepared and high oxygen pressure annealed samples, respectively. $Ru_{1.0}$ (○), $Ru_{0.9}Nb_{0.1}$ (□), $Ru_{0.9}Ti_{0.1}$ (◇) and $Ru_{0.9}V_{0.1}$ (▽).

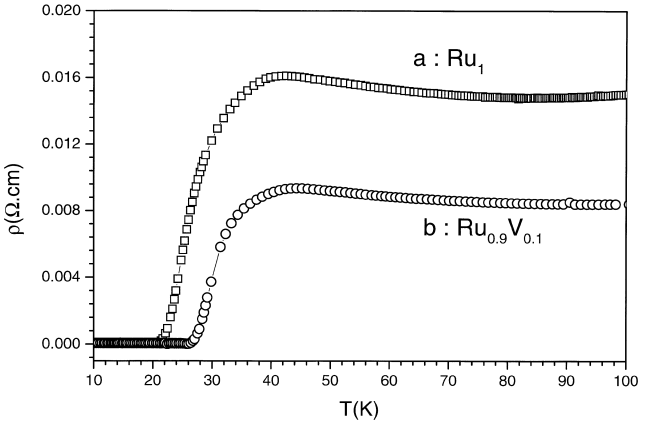

Fig. 9. T dependent resistivity (ρ) registered in the absence of external magnetic fields for two oxygen-pressure annealed samples, Ru-1212 (a) and $Ru_{0.9}V_{0.1}$-1212 (b).

creased by a factor of two as H_{ac} increases from 10^{-2} Oe to 1 Oe, and the superconductivity is totally suppressed at 3 Oe (Fig. 10). This strong sensitivity of the superconducting fraction to the application of low field has been previously explained by the unusual magnetic nature of the connecting layer of this 1212 cuprate. As the magnetic field increases, the magnetization in the ferromagnetic $SrRuO_3$ layer increases creating a large internal magnetic field which is the likely origin of the pair-breaking in the adjacent CuO_2 planes [7,8].

4. Discussion and concluding remarks

The present study of the $Ru_{1-x}M_xSr_2GdCu_2O_8$ '1212' samples, with M = Ti, V and Nb, and with $x \leq 0.2$, emphasizes the ability of this phase to incorporate foreign cations in its ruthenium layer. The chemical dopants strongly affect the magnetic properties of the Ru-1212 phase which are governed by the ferromagnetic RuO_2 planes. Complete solubility of Nb for Ru has been observed. The corresponding structural study will be reported elsewhere [16]. In accordance with their d^0 electronic configurations, only ~10% of Ti or Nb are sufficient to weaken the ferromagnetism of this phase. The most spectacular result is achieved with Ti, for which the magnetization at 5 K and in 55 kOe decreases by about 1 μ_B for $x = 0.15$, which indicates that the ferromagnetism of the RuO_2 layer is strongly suppressed.

The peculiar behavior of vanadium, which induces dramatic changes of the structure with a doubling of the c axis, is likely connected to its tetrahedral coordination similar to that already reported for V substituted Hg-based superconductors [17,18]. The ability of vanadium to adopt a $4+/5+$ mixed-valency probably explains the induced reinforcement of ferromagnetism and the small improvement in the T_{crit}. The RuO_2 layer is believed to act as a hole reservoir for the CuO_2 planes and the fact that chemical substitutions in this layer rapidly destroy the superconductivity for $x > 0.1$, demonstrates that this charge creation mechanism is very fragile.

Finally, the diamagnetism of Ru-1212 below T_c is very sensitive to the applied magnetic field as shown by the dramatic effect of the AC magnetic field magnitude on the superconducting diamagnetic fraction. This can explain why some groups have not observed superconductivity in the Ru-1212 phase. Therefore, we have checked the bulk superconductivity of this phase by measuring $\rho(T)$ curves in the presence of a large magnetic field of 10^4 Oe (Fig. 11). The resistive transition, though broadened by the field application as expected for a superconducting cuprate, is characteristic of a superconductor. Consequently, the suppression of the diamagnetism by small external applied magnetic fields is due to the large positive susceptibility values reached by the 2D ferromagnetic RuO_2 layers which overwhelm the diamagnetic signal.

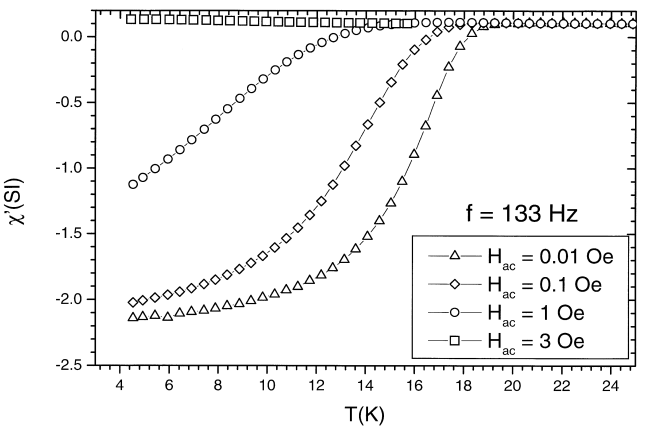

Fig. 10. χ' (T) curves registered for Ru-1212 (P_{O2} annealed) with the different H_{ac} values labeled in the graph ($f = 133$ Hz, $H_{dc} = 0$).

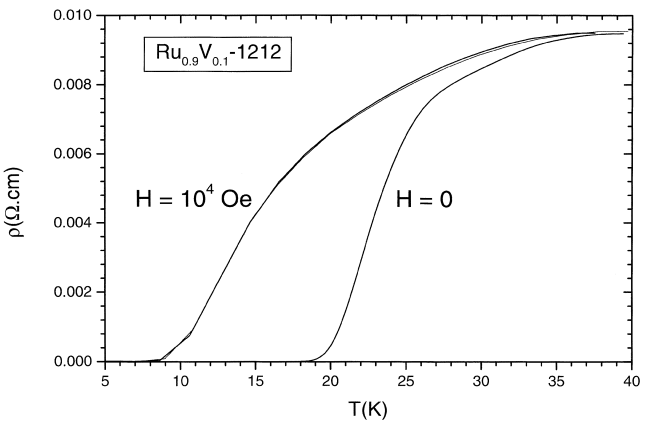

Fig. 11. $\rho(T)$ curves for the P_{O2} annealed $Ru_{0.9}V_{0.1}Sr_2GdCu_2O_8$ within $H = 0$ and $H = 10^4$ Oe. Note that the $\rho(T)$ curve in 10^4 Oe does not depend on the cooling process (zfc or fc curves).

Acknowledgements

The authors thank Carlton Washburn and Negar Mansourian-Hadavi for their help with specimen preparation. This work was supported by the National Science Foundation (Award No. DMR-9120000) through the Science and Technology Center for Superconductivity and made use of the Electron Probe Instrumentation Center supported by the National Science Foundation, at the Materials Research Center of Northwestern University (Award No. DMR-9632472).

References

[1] Basov DN, Timusk T, Dabrowski B, Jorgensen JD. Phys Rev B 1994;50:3511.
[2] Hardy V, Maignan A, Martin C, Warmont F, Provost J. Phys Rev B 1997;56:130.
[3] Villard G, Pelloquin D, Maignan A. J Appl Phys 1998;84:5080.
[4] Carrington A, Colson D, Dumont Y, Ayache C, Bertinotti A, Marucco JF. Physica C 1994;234:1.
[5] Kim DU, Gray KE, Kampwirth RT, Smith JC, Richeson DS, Marks TJ, Kang JH, Talvacchio J, Eddy M. Physica C 1991;177:431.
[6] Bauernfeind L, Widder W, Braun HF. Physica C 1995;254:151.
[7] McLaughlin AC, Zhou W, Attfield JP, Fitch AN, Tallon JL. Phys Rev B 1999;60:7512.
[8] Bernhard C, Tallon JL, Niedermayer Ch, Blasius Th, Gonik A, Brücher E, Kremer RK, Noakes DR, Stronach CE, Ansaldo EJ. Phys Rev B 1999;59:14099.
[9] Felner I, Asaf U, Reich S, Tsabba Y. Physica C 1999;311:163.
[10] Pringle DJ, Tallon JL, Walker BG, Trodahl HJ. Phys Rev B 1999;59:R11679.
[11] Attfield MP, Battle PD, Bollen SK, Kim SH, Powell AV, Workman M. J Solid State Chem 1992;96:344.
[12] Battle PD, Frost JR, Kim SH. J Mater Chem 1995;5:1003.
[13] Shannon RD. Acta Crystallogr Sect 1976;A32:751.
[14] Vybornov M, Perthold W, Michor H et al. Phys Rev B 1995;52:1389.
[15] Hellebrand B, Wang XZ, Steger PL. J Solid State Chem 1994;110:32.
[16] Malo S, Rijssenbeek JT, Ko D, Dravid VK, Maignan A, Poeppelmeier KR. To be published.
[17] Knizek K, Malo S, Michel C, Hervieu M, Maignan A, Raveau B. Physica C 1997;277:119.
[18] Villard G, Pelloquin D, Maignan A. Physica C 1998;307:128.
[19] Glazer AM. Acta Crystallogr Sect 1972;B28:3384.
[20] Rey MJ, Dehaudt Ph, Joubert J, Hewat AW. Physica C 1990;167:162.